THE JOURNAL OF PHYSICAL CHEMISTRY A

Article

pubs.acs.org/JPCA

On the Nature of Interactions of Radicals with Polar Molecules

Peter R. Tentscher*,† and J. Samuel Arey*,†,§

†Environmental Chemistry Modeling Laboratory, Swiss Federal Institute of Technology Lausanne, 1015 Lausanne, Switzerland

§Department of Environmental Chemistry, Swiss Federal Institute of Aquatic Science and Technology, 8600 Dübendorf, Switzerland

Supporting Information

ABSTRACT: Solvated radicals play an important role in many areas of chemistry, but to date, the nature of their interactions with polar solvent molecules lacks chemical interpretation. We present a computational quantum chemical analysis of the binding motives of binary complexes involving electron-poor and electron-rich radicals bound to water and hydrogen fluoride, considered here as model polar solvent molecules. By comparing the binding strengths of several open-shell and closed-shell complexes, in combination with natural localized molecular orbital analysis, we show that open-shell complexes can exhibit additional donor−acceptor interactions relative to analogous closed-shell systems. This may explain the unexpectedly large binding energies observed in some open-shell complexes. These exploratory results show that specific interactions in open-shell systems deserve more attention, and they imply that the quantum mechanical description of explicit solvent molecules needs to be considered carefully when designing simulation protocols for solvated radicals.

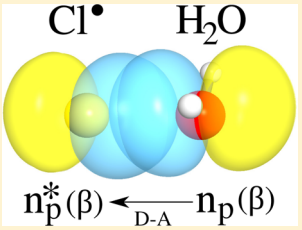

INTRODUCTION

Despite the wide relevance of solvated radicals in biological,[1] aquatic,[2] and atmospheric systems,[3−6] the nature of the interactions of radicals with polar solvent molecules has received limited study, compared to the analogous literature on closed shell intermolecular interactions. The simplest protosystem for the (micro)solvated phase is a binary complex between a radical and a solvent molecule. Open-shell complexes and closed-shell complexes share some types of binding motives: van-der-Waals interactions[7] and hydrogen bonds.[8,9] However, unlike closed-shell systems, radicals have been reported to engage in an interaction termed a "hemibond" or "2-center-3-electron bond",[10] which has also been interpreted as a single electron covalent bond.[11] Analogous to the 2-center-3-electron interactions, 2-center-1-electron complexes have been reported as well.[12] This type of interaction has been studied in several reports,[10−16] but the chemical interpretation of the interaction was limited to cationic or anionic binary complexes, most of which were homodimeric. Maity[16] reported computed Mayer bond orders for many heterodimeric cationic radical complexes. In his results, not all complexes exhibited a bond order close to 0.5, which should be expected for hemibonded interactions. For some complexes, he found bond orders close to zero despite a relatively high binding energy. For example, for $H_2O\cdots SH_2^{\bullet+}$ Maity reported a bond order of 0.16 and a binding energy of 91 kJ mol^{-1}. Some other studies have reported radical cations complexed by a single water molecule,[13,17−21] and in these cases, the term "hemibond" was adapted without revisiting the nature of the interaction.

In separate works, alkali metal−water complexes have received ample attention (see, e.g., Hertel[22] and Morokuma[23])) and sodium doping of clusters of various polar molecules is emerging as a way to softly ionize these clusters.[24−27] These studies were mostly concerned with ionization energies and binding energies in clusters of varying size. In this context, the interactions of $Na^{\bullet}$ with polar solvent molecules (H_2O, NH_3, HAc) have been referred to as dispersive.[25,27] However, in earlier works, alkali atoms were found to bind strongly to single water molecules or clusters of polar solvent molecules with both experimental and computational techniques.[28,29] For example the binding energies of $H_2O\cdots Na^{\bullet}$ and $H_2O\cdots Li^{\bullet}$ were previously reported as −25 kJ mol^{-1} and −45 kJ mol^{-1}, respectively.[29] Additionally, computations suggest severe delocalization of the unpaired electron onto surrounding water molecules for $(H_2O)_n\cdots Na^{\bullet}$.[30]

These inconsistent descriptions of the interactions of radicals with polar solvent molecules may be related to the limited chemical insight into the underlying binding motives. In particular, we have not found work which has interpreted these binding motives from a chemical point of view, for complexes of polar solvent molecules bound to diverse types of neutral and ionic, electron-rich, and electron-poor radicals. However, it is reasonable to suspect that these interactions are worth exploring. In a recent study, the Head-Gordon group reported on ionic radical-molecule complexes in the context of their similarity to transition states of bond-making/bond-breaking reactions.[31] These authors concluded that additional or stronger charge-transfer interactions may arise in open-shell complexes compared to similar closed-shell complexes, justified by differences in orbital overlap between the closed-shell and the open-shell aggregates.

In the present work, we explored the nature of the binding in selected radical−solvent binary complexes. We recently reported benchmark binding energies for a chemically diverse set of such complexes.[32] Here, we focused on qualitative

Received: July 16, 2013
Revised: October 14, 2013
Published: November 13, 2013

Table 1. Binding Energies ([kJ mol^{-1}]) and Interfragment Distances (Å) of Binary Open-Shell Complexes and Analogous Closed-Shell Complexes

								spin population[d]			
no.	complex	D_e[a]	D_e[HF]	ΔD_e[corr]	D_0[b]	r_e[c]	B_{AB}	SP_A	SP_B	ref	analogues[e]
Electron-deficient radical complexes											
1	$H_2O\cdots F^{\bullet}$	−16.0	27.5	−43.6	−11.8	2.118	0.22	0.12	0.88	32	
2	$H_2O\cdots Cl^{\bullet}$	−15.4	5.8	−21.3	−12.0	2.604	0.14	0.07	0.93	32	**2.1**, **6**, **7**
3	$H_2O\cdots Br^{\bullet}$	−15.1	5.6	−20.4	−12.0	2.705	0.12	0.06	0.94	32	
4	$H_2O\cdots NH_3^{\bullet+}$	−76.6	−57.1	−19.7	−67.6	2.323	0.15	0.08	0.92	32	
5	$HF\cdots CO^{\bullet+}$	−122.2	−85.4	−36.6	−115.2	1.799	0.41	0.18	0.82	32	**8**
Closed-shell CT complexes analogous to species **2** and **5**											
6	$H_2O\cdots Cl_2$	−12.2	−2.6	−9.4	n.a.	2.786	0.02			this work[f]	
7	$H_3N\cdots Cl_2$	−20.1	−0.6	−19.5	n.a.	2.633	0.07			this work[f]	
8	$HF\cdots CF^{+}$	−67.7	−58.7	−9.0	−62.6	2.116	0.12			this work[f]	
Water-main group metal complexes											
9	$H_2O\cdots Li^{\bullet}$	−51.8	−41.8	−10.1	−47.5	1.888	0.06	0.07	0.93	32	
10	$H_2O\cdots Na^{\bullet}$	−23.8	−17.5	−6.5	−21.5	2.338	0.06	0.04	0.96	this work[f]	**10.1**, **10.2**
11	$H_2O\cdots Be^{\bullet+}$	−268.3	−263.6	−5.0	−258.6	1.547	0.16	0.06	0.94	32	**12**
12	$H_2O\cdots Li^{+}$	−144.6	−148.9	4.2	−136.7	1.885	0.01			this work[f]	
13	$H_2O\cdots Al^{\bullet}$	−31.6	−16.3	−15.5	−28.5	2.216	0.08	0.01	0.99	32	
Water-noble gas complexes[g] mimicking species **2** and **10**											
2.1	$H_2O\cdots Ar$	−1.1	1.6	−2.7	n.a.	3.554				this work[f,g]	
10.1	$H_2O\cdots Ar$	−1.1	2.2	−3.3	n.a.	3.422				this work[f,g]	
10.2	$H_2O\cdots Kr$	−1.5	2.6	−4.1	n.a.	3.473				this work[f,g]	
H-bonded complexes											
14	$FH\cdots BH_2^{\bullet}$	−16.9	−7.5	−9.4	−9.0	2.221	0.07	0.05	0.95	32	**18**
15	$FH\cdots NH_2^{\bullet}$	−41.0	−32.4	−8.7	−29.5	1.750	0.08	0.00	1.00	32	**17**, **19**
16	$FH\cdots OH^{\bullet}$	−24.8	−17.8	−7.1	−17.6	1.813	0.05	0.00	1.00	32	**18**, **19**
17	$FH\cdots NH_3$	−55.4	−46.5	−9.0	n.a.	1.697	0.10			59	
18	$FH\cdots FH$	−19.3	−16.0	−3.4	n.a.	1.824	0.02			59	
19	$FH\cdots OH_2$	−37.4	−31.9	−5.5	n.a.	1.714	0.05			59	

[a]Theoretical best estimates of electronic binding energies. [b]Best estimates of total binding energies at 0 K, including zero-point vibrational energies. [c]Equilibrium distance between the closest nuclei of the two fragments. [d]Natural spin density summed over all nuclei of the polar molecule **A** and the radical **B**. [e]Indices of comparable isoCoulombic complexes. [f]Computational protocol from Tentscher and Arey,[32] see Supporting Information for details. [g]Binding energy of a partially optimized geometry, see text for details.

differences between electron-rich and electron-poor radical binding modes, as well as on differences between radical−solvent complexes and analogous isoCoulombic closed-shell complexes. The systems under consideration are summarized in Table 1 and Figure 1. We categorized them qualitatively on the basis of the following considerations: (1) How do these radical−solvent interactions compare to those of analogous closed-shell complexes in strength and covalent character? (2) Which types of orbitals could be responsible for a possible partial donor−acceptor nature of the interaction?

We analyzed binding energies, spin densities, bond orders, and natural localized molecular orbitals of selected radical complexes and their closed-shell counterparts. We found indications of a partly covalent character in the binding of electron-poor and electron-rich radicals to single polar solvent molecules in cases where the unpaired electron is in direct contact with water lone pairs. H-bonded complexes, where the radical center acts as an H-bond acceptor, were found not to differ in binding motive from closed-shell hydrogen-bonded complexes.

COMPUTATIONAL METHOD

Selection of Complexes. We considered a diverse set of 12 complexes of small radicals with a single molecule of either water or HF as model solvent, which are numbered in Table 1. They were selected to allow two types of comparisons: (a) comparisons between electron-poor and an electron-rich radicals interacting with lone electron pairs of solvent, and (b) comparisons between open-shell molecules and similar closed-shell molecules interacting with polar solvent. The focus was on complexes having direct interactions of the unpaired electron with the solvent molecule.

The first group contains neutral and cationic electron-deficient radicals (**1**−**5** in Table 1).[33] $H_2O\cdots Cl^{\bullet}$ (**2**) was analyzed in detail, and we included closed-shell complexes which resemble $H_2O\cdots Cl^{\bullet}$ (**2**) in either geometry or binding energy for comparison (**2.1**, **6**, **7**). The second group consists of electron-rich main group metal atoms, where the metal atom contacts the oxygen of H_2O (**9**−**11**, **13**). For $H_2O\cdots Na^{\bullet}$ (**10**), analogous closed-shell water-noble gas complexes, constrained to similar geometries, were included (**10.1**, **10.2**). The third group consists of H-bonded complexes with a spin-bearing center as H-bond acceptor (**14**−**16**). We also considered closed-shell H-bonded complexes having similar binding energies (**17**−**19**), for comparison.

The open-shell complexes considered were selected to have low spin contamination ($\langle S^2\rangle$ of the UHF reference ≤0.76), with the exception of $H_2O\cdots Al^{\bullet}$ ($\langle S^2\rangle$ = 0.79) and $Al^{\bullet}$ ($\langle S^2\rangle$ = 0.77) as well as $HF\cdots CO^{\bullet+}$ ($\langle S^2\rangle$ = 0.86) and $CO^{\bullet+}$ ($\langle S^2\rangle$ = 0.97). For $HF\cdots CO^{\bullet+}$, where the cited reference binding energies correspond to ROHF-based results, we demonstrated previously[32] that the inclusion of the post-CCSD(T)

dx.doi.org/10.1021/jp407041e | J. Phys. Chem. A 2013, 117, 12560−12568

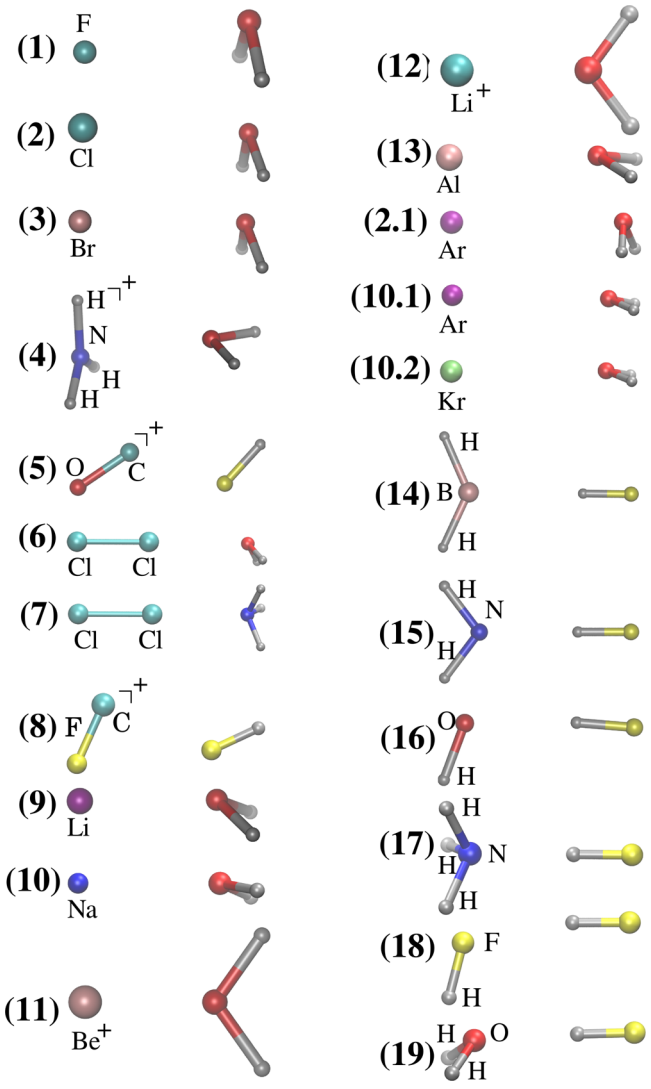

Figure 1. Conformations of all complexes, listed by numbering given in Table 1.

excitations in the presently used protocol lowers the influence of the (spin-contaminated) reference on the binding energies to 0.3 kJ mol^{-1}. Thus, we considered UHF references to be sufficient for the additional benchmark binding energies presented here.

Characterization of Complexes. We used different approaches to characterize the binding motives of both open-shell and closed-shell complexes. First, we compared the computed benchmark binding energies of open-shell complexes to those of similar closed-shell complexes. We also considered operationally defined components of the electronic binding energy, that is, the Hartree−Fock binding energy, D_e [HF], and contributions from the coupled cluster treatment of electron correlation, ΔD_e [corr]. D_e [HF] and ΔD_e [corr] do not include relativistic contributions to the binding energy, whereas D_e and D_0 include relativistic contributions where available. Accordingly, D_e [HF] and ΔD_e [corr] do not exactly sum up to D_e . For selected cases ($H_2O\cdots Cl^\bullet$ and $H_2O\cdots Na^\bullet$), we evaluated the binding energies of complexes where the radical was replaced by a noble gas atom (Ar or Kr), at geometries with reoptimized oxygen-noble gas distances but otherwise frozen coordinates. This should allow a meaningful estimate of the magnitudes of dispersion and Debye interactions in the corresponding radical complexes.

Second, we visualized the spin density for all of the complexes, and we show these results for selected cases. Third, we performed natural bond orbital (NBO) and natural localized molecular orbital (NLMO) analysis.[34−38] On the basis of natural population analysis (NPA),[39] we also report spin-corrected Mayer bond orders[40] (in the NAO basis) between the two closest nuclei of the respective fragments, denoted B_{AB},[41] and natural spin density populations summed over the fragments. Differences between the localized NBOs and the semilocalized NLMOs, that is, NLMO "delocalization tails", arise from donor−acceptor interactions between occupied and unoccupied NBOs. We focus our analysis on the extent of intermolecular delocalization of the NLMOs and the types of NBOs involved in those delocalizations, but it should be kept in mind that the more traditional perturbative estimates of NBO donor−acceptor interactions[36−38,34] give similar information in terms of the involved orbitals and the strength of the interaction. Although these perturbative estimates were also analyzed in the course of the present work, we chose not to report them as they yielded conclusions redundant with those drawn from NLMO analysis.

Our approach is in the same spirit as the concept of orbital mixing in qualitative MO theory of covalent bonds:[42] the localized NBOs on different fragments/molecules are linearly combined to form bonding and antibonding NLMOs. For the analysis of the radical−solvent interactions, we operationally define the term *covalent character* as the extent of interfragment delocalization of the NLMO; that is, a squared coefficient of the NBO entering the linear combination with a value smaller than 1 is considered a manifestation of *covalent character*. However, it should be kept in mind that this simply corresponds to NBO−NBO donor−acceptor interactions. More details on this approach are given in the Supporting Information. In the somewhat simplified picture used in the present exploratory study, we did not discriminate between possible types of interactions (dative, ionic, and covalent)[34] within the NBO framework. Nevertheless, we believe the above definition of covalent character to be a meaningful descriptor for the *relative covalency* of intermolecular interactions, if donor−acceptor interactions of the same type are compared. For radicals, NBO/NLMO analysis is performed separately for the two spin manifolds ("different spin different hybrids" (DSDH)[36,43]).

Computational Details. Benchmark binding energies were computed with a protocol described elsewhere;[32] detailed results are given in the Supporting Information (SI). In brief, all-electron CCSD(T)[44]/aug-cc-pVTZ[45,46] was used for geometry optimizations and harmonic frequency calculations. Electronic energies were evaluated using basis-set extrapolated CCSD(T)/aug-cc-pV{4,5}Z[45,46] with corrections for core−valence correlation (CCSD(T)/aug-cc-pCVQZ[47]) and higher excitations (CCSDT[48]/cc-pVTZ, CCSDT(Q)[49]/cc-pVDZ), and relativistic corrections (MVD2[50]/CCSD(T) and ZORA-DFT[51]) in some cases.

For some complexes of water with noble gas atoms (**2.1**, **10.1**, **10.2** in Table 1), we used geometries that do not correspond to minimum structures. In these cases, we used the geometry of a corresponding radical complex (**2**, **10**) as a starting geometry, but we replaced the radical with a noble gas atom. Subsequently, only the oxygen-noble gas distance was optimized while all other internal coordinates remained constant.

dx.doi.org/10.1021/jp407041e | J. Phys. Chem. A 2013, 117, 12560−12568

We report the contribution to the electronic binding energy of the Hartree−Fock component, D_e[HF], and the change in binding energy arising from the coupled cluster treatment of electron correlation, ΔD_e[corr]. The Hartree−Fock result corresponds to the single-determinantal, mean-field molecular orbital approach. Consequently, ΔD_e[corr] can account for both dispersive forces and other effects of dynamical and nondynamical electron correlation beyond the HF model and should not be equated to dispersion.

Spin densities were visualized from the correlated CCSD-(T)/aug-cc-pVTZ electronic structure as computed with CFOUR,[52] using MOLDEN 5.0.[53] DFT calculations were conducted with the Gaussian 09 rev. B.1 electronic structure program,[54] applying a pruned (99,590) integration grid and Dunning's aug-cc-pVTZ basis[46,55] with the BHandHLYP[56] functional. Natural bond orbital (NBO) analysis[36] was conducted with the NBO 5.0 program suite.[57] We chose BHandHLYP/aug-cc-pVTZ densities for NBO analysis because good performance has been reported for this functional in previous studies on radical complexes,[13,15] and also because this method performed well in our own assessment.[32] The NBO results were checked for qualitative agreement with an NBO analysis of the CCSD/aug-cc-pVDZ density as implemented in Q-Chem 4.0.[58] We prefer to report the NBO results based on DFT densities rather than CCSD densities because the former allow meaningful one-electron energies to be assigned to the natural orbitals.[34] Mayer bond indices and Wiberg bond indices were computed in the NAO basis from RO-BHandHLYP/aug-cc-pVTZ orbitals. In the Supporting Information, we briefly introduce some concepts of NBO analysis, which is described comprehensively elsewhere.[34−36,38]

RESULTS AND DISCUSSION

Electron-Deficient Radicals. For this category of systems (**1**−**5** in Table 1), binding energies suggest a covalent contribution to the binding. The neutral radical halogen−water complexes (**1**−**3**) exhibit binding energies ranging from −11.0 to −15.9 (Table 1). For these systems, binding energies are comparable to analogous closed-shell CT complexes ($H_2O\cdots Cl_2$, $H_3N\cdots Cl_2$). In contrast, the analogous closed-shell complex between H_2O and the Ar atom (**2.1**), in a conformation similar to $H_2O\cdots Cl^\bullet$ (**2**), exhibits a much smaller binding energy than **2** despite the similar size of $Cl^\bullet$ and Ar. (Similarly, for the global minimum geometry of the $H_2O\cdots Ar$ complex, where Ar acts as an H-bond acceptor, the binding energy is merely −1.7.[60]) The charged $HF\cdots CO^{\bullet+}$ system exhibits twice the binding energy of the analogous isoCoulombic closed-shell $HF\cdots CF^+$ complex (Table 1), which cannot be explained by electrostatic differences.[61] In this case, the C−F distance is significantly shortened in $HF\cdots CO^{\bullet+}$ compared to $HF\cdots CF^+$, which may additionally indicate partial covalency of the interaction.

The uncharged radical halogen−water complexes (**1**−**3**) exhibit a repulsive HF component of the binding energy, potentially indicating that the binding is not of electrostatic nature (halogen atoms do possess a quadrupole moment). This is offset by the correlation contribution ΔD_e [corr] to the binding energy, which is unusually strong compared to, for example, H-bonded systems (**14**−**19**), and which cannot be attributed to dispersion alone. For further comparison, in the $H_2O\cdots Cl_2$ complex, which is analogous to $H_2O\cdots Cl^\bullet$ and which could be arguably described as halogen-bonded or charge-transfer (CT), D_e [HF] was not found repulsive. Interestingly, if H_2O is replaced by the better electron donor NH_3 to form the $H_3N\cdots Cl_2$ CT-complex, the distribution of D_e [HF] and ΔD_e [corr] is again similar to the situation in $H_2O\cdots Cl^\bullet$.

Examination of the spin densities showed that for all systems involving electron-deficient radicals, the unpaired electron is significantly delocalized onto the solvent molecule, indicative of a covalent 1e-interaction (see Figure 3 for a representative example). Taken together, the binding energy and spin density data suggest that the binding in the electron-deficient radical complexes may be partly covalent. For radical halogen−water complexes, binding energies are comparable to analogous closed-shell CT complexes ($H_2O\cdots Cl_2$, $H_3N\cdots Cl_2$). To further explore this contention, we considered NBO/NLMO results.

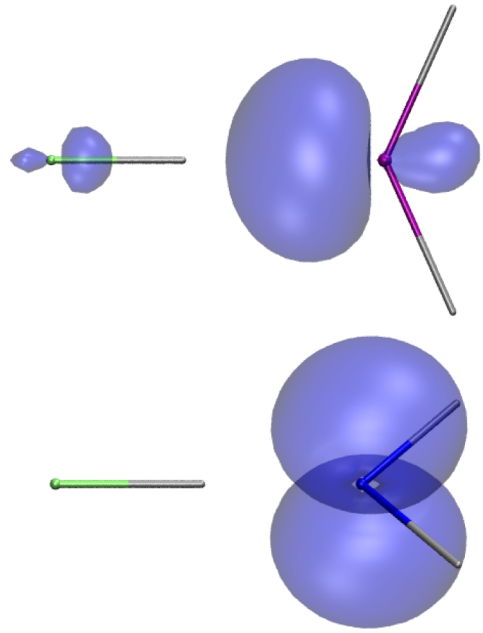

Figure 2. Spin density isosurfaces (isovalue 0.02 $e^-Å^{-3}$) from CCSD(T)/aug-cc-pVTZ electronic structure. Spin donation due to the n_{sp}-SOMO in the bond axis ($FH\cdots BH_2^\bullet$, top), and absence of spin donation in case of a n_p-SOMO ($FH\cdots NH_2^\bullet$, bottom).

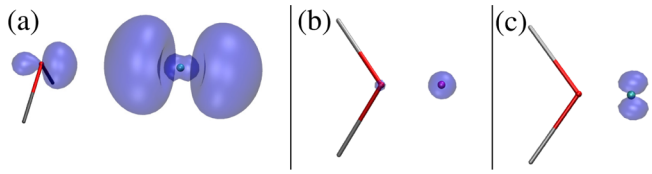

Figure 3. Spin density isosurfaces (isovalue 0.02 $e^-Å^{-3}$) from CCSD(T)/aug-cc-pVTZ electronic structure. (a) Strong mixing of the O_{sp} lone pair with n^*_{Cl} in $H_2O\cdots Cl^\bullet$, (b) weak mixing of the SOMO with a Ry^*_O orbital for $H_2O\cdots Li^\bullet$, and (c) no spin transfer for $H_2O\cdots Al^\bullet$.

The NBO/NLMO interpretation of the binding in the studied electron-deficient radical complexes is a donor−acceptor interaction, with qualitatively similar binding motives observed throughout. We show detailed results for $H_2O\cdots Cl^\bullet$, which we considered representative (Figure 4). For alpha electrons, no orbital mixing between the monomer NBOs is observed. For beta electrons, the n_p orbital of water strongly mixes with the n^*_p "electron hole" of chlorine. We interpret that the large energy gain from mixing is offset by a strong Pauli repulsion of the alpha electrons, which results in the observed weak binding energy.[62] In the NBO framework, this 2c3e-

dx.doi.org/10.1021/jp407041e | J. Phys. Chem. A 2013, 117, 12560−12568

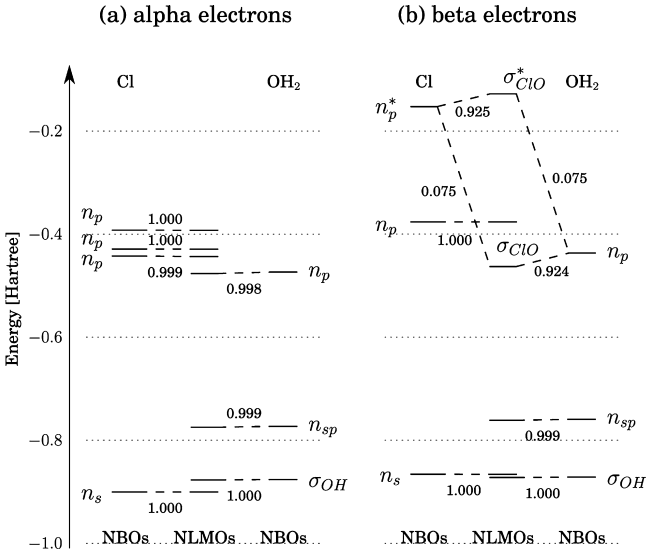

Figure 4. NBO to NLMO mixing based on the BHandHLYP/aug-cc-pVTZ density of the $H_2O\cdots Cl^{\bullet}$ complex. Numbers on dashed lines are the squared coefficients of the NBO contribution to the NLMOs rounded to three decimal places. (a) No delocalized NLMOs are found for alpha electrons, whereas (b) a single NLMO spanning the two fragments is found for beta electrons.

interaction can be described in two ways: the best description (99.69% Lewis-character) is a donor−acceptor complex with a strong beta spin-only $n_p \rightarrow n_p^*$ donation; the other description is a single electron σ_{ClO} bond (beta spin) with a lower Lewis-character (98.70%).

A similar situation arises for the strongly bound $HF\cdots CO^{\bullet+}$ complex: no interfragment orbital mixing occurs for alpha electrons, and a n_p NBO of HF mixes with the n* of $CO^{\bullet+}$ for beta electrons. We rationalize this strong bond (relative to $HF\cdots CF^+$) qualitatively as a better overlap of the n_p and n* orbitals compared to the $n_p-\pi^*$ interaction in the closed shell case (not shown).

Comparative NLMO analysis of the e-deficient radical complexes suggests covalent character for all of these systems, although the extent of covalent character varies significantly among the complexes studied. The squared coefficients with which the parent NBOs (the β lone pairs) enter the delocalized NLMOs deviate significantly from a value of 1.0, which arises from the contributions of the n_p^* "electron hole" of the radicals: 0.780 ($HF\cdots CO^{\bullet+}$), 0.860 ($H_2O\cdots F^{\bullet}$), 0.921 ($H_2O\cdots NH_3^{\bullet+}$), 0.924 ($H_2O\cdots Cl^{\bullet}$), and 0.935 ($H_2O\cdots Br^{\bullet}$). For the neutral complexes, the order (F > Cl > Br) is in qualitative agreement with the decreasing orbital overlap that can be expected from the increasing diffuseness of acceptor orbitals with increasing halogen atom size. In the NBO picture, the two systems with the strongest delocalizations ($HF\cdots CO^{\bullet+}$ and $H_2O\cdots F^{\bullet}$) are best described with a strongly polar single electron bond rather than with a donor−acceptor interaction, in agreement with Bickelhaupt's interpretation of the hemibond.[11] In contrast, the NBO picture of the more weakly delocalized systems could be seen as the open-shell, single electron analogue to closed-shell CT complexes.

We compared the covalent character of these open-shell systems to that of closed-shell CT complexes where electron donation into antibonds is present. For $HF\cdots CF^+$, $H_3N\cdots Cl_2$, and $H_2O\cdots Cl_2$, the squared coefficients are 0.971, 0.966, and 0.990, where the deviation from 1 is attributed to the π^*_{CF} orbital of CF^+ and the σ^*_{ClCl} of Cl_2, respectively. Compared to closed shell CT complexes, the single-electron interactions in the open-shell complexes bear more covalent character throughout.

The complex between benzene radical cation and H_2O (as well as other nucleophiles) in the "top" orientation,[31] studied with a block-localized wavefunction approach in a recent contribution,[31] also falls in the category of electron-deficient radicals interacting with polar solvent molecules. In their complementary occupied-virtual pairs (COVPs) analysis, conceptually similar to NBO donor−acceptor interactions, these authors found a significantly stabilizing CT interaction between the water n_{sp} and an unoccupied $\beta-\pi$ orbital of the ionized benzene ring. Only a weak CT interaction was reported for α electrons. These findings are in qualitative agreement to the results reported here, and they also illustrate that by a methodology independent from the NBO framework, strikingly different CT interactions are again observed to arise in the respective spin manifolds.

In summary, the electron-deficient radicals accept electron density from the polar solvent molecules through their n* orbitals. This interpretation is supported by stronger binding relative to analogous closed-shell complexes, delocalized spin densities, and NLMO analysis. Similar binding motives of electron donation into unoccupied n* orbitals (but for both α and β electrons at the same time) can be found in transition metal complexes.[34]

Electron-Rich Main Group Metals. For complexes of electron-rich main group metal radicals with water molecules (**9**−**11**, **13**) binding energies also suggest significant covalent character. The neutral $H_2O\cdots Li^{\bullet}$, $H_2O\cdots Na^{\bullet}$, and $H_2O\cdots Al^{\bullet}$ complexes exhibit binding energies of −51.8, −23.8, and −31.6 kJ mol^{-1}, respectively. By comparison, van-der-Waals complexes of water with Ne and Ar (**10.1**, **10.2**), which mimic $H_2O\cdots Na^{\bullet}$, are only very weakly bound. This indicates that additional intermolecular interactions are present in the neutral radical complexes. Similarly, the charged $H_2O\cdots Be^{\bullet+}$ complex is bound about twice as strongly as the analogous isoCoulombic $H_2O\cdots Li^+$ complex. In this case, the $Be^{\bullet+}-O$ distance is shortened significantly compared to Li^+-O, suggesting covalent contributions to the binding. The contribution to the binding energy due to electron correlation for these systems is in the same range as for hydrogen-bonded systems (−3.4 to −7.4 kJ mol^{-1}), with the exception of $H_2O\cdots Al^{\bullet}$, for which the correlation contribution is slightly higher (−15.5 kJ mol^{-1}).

The binding motives of the electron-rich complexes differ from those of the electron-poor complexes studied here. For $H_2O\cdots Li^{\bullet}$, $H_2O\cdots Na^{\bullet}$, and $H_2O\cdots Be^{\bullet+}$, we observed a small amount of spin density localized on the H_2O fragment (Figure 3). For $H_2O\cdots Al^{\bullet}$, however, the spin density assumes the shape of a p-type orbital perpendicular to the bond axis, and is thus likely not involved in the interaction. The computed binding energies of the neutral complexes are too large to be explained by dispersion alone. These data, as well as the large binding energy of $H_2O\cdots Be^{\bullet+}$ relative to $H_2O\cdots Li^+$, raise the question of whether these complexes are held together by donor−acceptor interactions. To explore this question, we turned to NBO/NLMO analysis.

The NLMO interpretation of the $H_2O\cdots Li^{\bullet}$ complex suggests interfragment delocalizations in both the α and β spin manifolds (Figure 3 and 5). The α lone electron (n_s) of $Li^{\bullet}$ delocalizes into an oxygen Rydberg orbital of water (Ry^*_{sp}), and to a lesser extent into the σ^*_{OH}-antibonds of water. The β n_{sp} of

dx.doi.org/10.1021/jp407041e | J. Phys. Chem. A 2013, 117, 12560−12568

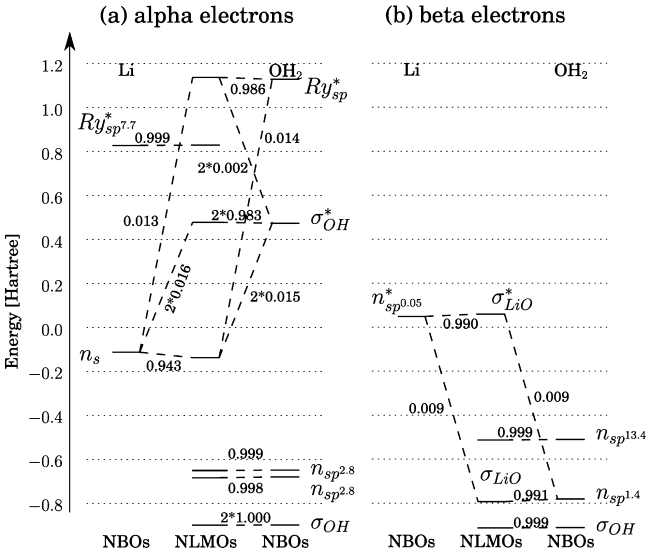

Figure 5. NBO to NLMO mixing based on the BHandHLYP/aug-cc-pVTZ density of the $H_2O\cdots Li^{\bullet}$ complex. Numbers on dashed lines are the squared coefficients of NBO contribution to the NLMOs rounded to three decimal places. (a) The lone electron (alpha spin) delocalizes into a Rydberg orbital of the water oxygen, as well as the two σ^*_{OH} antibonds of water. (b) In the beta spin manifold, a water lone pair is slightly delocalized into the unoccupied s-orbital of $Li^{\bullet}$, much like in the $H_2O\cdots Li^{+}$ complex.

water delocalizes into the n_s^* of $Li^{\bullet}$, analogous to the $H_2O\cdots Li^{+}$ complex. (Similar results for $H_2O\cdots Na^{\bullet}$ and $H_2O\cdots Be^{\bullet+}$ are not shown.) The large binding energy of **9**, **10** compared to the electron-deficient hemibonded complexes, despite the small orbital mixing, is likely to be explained by a lower Pauli repulsion and a "donation−back-donation" binding motive. Such bidirectional bonding occurs in transition metal complexes, for example in nickel−CO complexes (σ-bonding, π-backbonding),[34] but proceeds through the conventional electron pair donor−acceptor interactions.

Orbital mixing in $H_2O\cdots Be^{\bullet+}$ is qualitatively similar to that observed in $H_2O\cdots Li^{\bullet}$, but the delocalization of the water lone electron (β-spin) is much more pronounced. The low orbital energy of the beta n_s^* orbital in the $H_2O\cdots Be^{\bullet+}$ system likely contributes to the strong binding in this complex. Compared to $H_2O\cdots Li^{\bullet}$, the $Be^{\bullet+}$ n_s^* orbital is energetically closer to the n_{sp} water lone pair, which allows for a more favorable donor−acceptor interaction. For $H_2O\cdots Na^{\bullet}$, the smaller binding energy compared to $H_2O\cdots Li^{\bullet}$ may be attributed to smaller orbital overlap of the H_2O-centered NBOs with the more diffuse orbitals of $Na^{\bullet}$.

For $H_2O\cdots Li^{\bullet}$, $H_2O\cdots Be^{\bullet+}$, and $H_2O\cdots Na^{\bullet}$, the squared coefficients of the α n_s NBOs entering the NLMOs are 0.943, 0.967, and 0.968, respectively, mainly due to delocalization into a Rydberg orbital of oxygen. For the β spin orbitals, the squared coefficients of the water lone electron NBO are 0.991, 0.963, and 0.992, respectively, which is caused by delocalization into the n_s^* of the metal. This provides further evidence that this β electron interaction is responsible for the stronger binding of $H_2O\cdots Be^{\bullet+}$ compared to $H_2O\cdots Li^{+}$. For $H_2O\cdots Al^{\bullet}$, delocalization found by NLMO analysis is the same for both alpha and beta electrons, where the n_{sp} of water donates to the n_p^* of Al that lies in the bond axis (Figure 3), much like in transition metal complexes. The covalent character of $H_2O\cdots Al^{\bullet}$ is comparable to that of closed shell CT complexes, with the water lone electrons entering the 1e-NLMOs with squared coefficients of 0.985 and 0.984 for α and β electrons, respectively. In summary, we found an α-donation β-back-donation binding motive for s-block metals complexed to water, whereas elemental aluminum is found to accept electron density in its unoccupied *pair* of p-type spin orbitals, which may be compared to metal−ligand complexes of d-block elements.

Open-Shell Hydrogen-Bonded Systems. Open-shell hydrogen bonded systems (**14**−**16**) exhibit binding strengths similar to analogous closed-shell hydrogen bonded systems (**17**−**19**), and binding motives are similar as well. In the NBO picture, a closed-shell H-bond is, in addition to electrostatic interactions, described by a donor−acceptor component, indicative of the partial covalency[63] of the hydrogen bond. There, a lone *pair* of the H-bond acceptor donates into the $\sigma^*_{OH}/\sigma^*_{FH}$ antibond of the H-bond donor. This is also the case for most of the open-shell hydrogen bonded systems considered here: the unpaired electron is usually localized in a n_p orbital perpendicular to the bond axis, and it does not take part in the donor−acceptor interaction. This observation is in agreement with a previous detailed study on hydrogen bonding of the hydroperoxy radical ($HOO^{\bullet}$).[64] We did not observe differences in the magnitude of NLMO interfragment delocalization between closed-shell and open-shell H-bonded complexes of similar strength. However an exception is $FH\cdots BH_2^{\bullet}$, where the n_p orbital remains unoccupied, and where the unpaired electron (n_{sp}) lies in the bond axis (Figure 2). Hence, in this system, the donor−acceptor nature of the H-bond can involve the unpaired electron, yielding a physical manifestation in the spin density. For the weak $HOH\cdots CH3^{\bullet}$ complex, in which the unpaired electron also lies in the bond axis, such a "spin density transfer" was not observed based on visual inspection of the spin density (data not shown). However, recently reported COVP results of the $(H_3C)_3C^{\bullet}\cdots HOH_2^{+}$ H-bonded complex[31] suggest a large α-spin only CT component, so that a spin-density transfer may be expected, analogous to what we report for $FH\cdots BH_2^{\bullet}$. In contrast to the hydrogen bonding of the hydroperoxy radical,[64] we did not observe an increased strength of the radical hydrogen bonds compared to closed-shell analogues (**17**−**19**). This is attributed to the fact that in the complexes of the hydroperoxy radical, the radical acts (also) as an H-bond donor, and in that system the electronic effects were found to enhance the H-bond donating capacity compared to H_2O_2.[64]

■ CONCLUSION

Most of the electron-deficient 2c3e complexes and electron-rich water−metal complexes studied here are best explained as charge-transfer or donor−acceptor complexes, where the CT interaction is only present in one of the respective spin manifolds. However, these 1e-CT interactions are more strongly delocalized than the 1e component of closed-shell H-bonds or closed-shell CT complexes. The electron-deficient complexes investigated here are additionally characterized by a strong contribution of electron correlation to the binding energy, compared to the other types of complexes studied here. In contrast, most open-shell H-bonded complexes, as well as the $H_2O\cdots Al^{\bullet}$ complex, do not differ in binding motive from corresponding closed-shell complexes.

Computed Mayer bond indices are in line with the conclusions inferred from the other approaches used in the present work. B_{AB} values of the electron-deficient radical complexes considered here are far from the value of 0.5 that

dx.doi.org/10.1021/jp407041e | J. Phys. Chem. A 2013, 117, 12560−12568

should be expected for hemibonded systems,[16] with the exceptions of HF···$CO^{\bullet+}$ and (arguably) H_2O···$F^{\bullet}$, both of which are also best described with a single electron bond in the NBO framework. However, bond order values of the electron-deficient radical systems are all substantially different from zero, and they indicate slightly increased delocalization compared to the analogous closed-shell CT complexes studied here. These results are consistent with findings by Maity,[16] who studied a set of eighteen electron-poor cationic radical complexes. For some systems, Maity found bond order values ranging from 0.34 to 0.55 and correspondingly large spin density transfer, whereas the remaining systems had lower bond order values (0.0 to 0.16) and exhibited relatively small spin density transfer. In summary, the bond indices and spin populations support the conception that the H_2O···$Cl^{\bullet}$, H_2O···$Br^{\bullet}$, and H_2O···$NH_3^{\bullet+}$ complexes studied here are CT complexes, whereas HF···$CO^{\bullet+}$ and H_2O···$F^{\bullet}$ could be best described as "hemibonded". Similar conclusions can be drawn for the bond orders of the water-metal complexes. The bond orders of H_2O···$Li^{\bullet}$ and H_2O···$Na^{\bullet}$ are small compared to those of electron-deficient complexes but still comparable to the bond orders of hydrogen bonds. However, the open-shell water-S-block metal complexes exhibit a significant bond order not only between oxygen and the metal atom, but also between the metal and hydrogen. If we sum the bond orders of the metal interactions with both O and H, this would result in increases of B_{AB} to 0.10 and 0.08 in H_2O···$Li^{\bullet}$ and H_2O···$Na^{\bullet}$, respectively.

We have shown that radical−solvent complexes can be bound more strongly than analogous isoCoulombic closed-shell complexes. In the NBO/NLMO picture, the studied complexes exhibit donor−acceptor interactions which render them at least as covalent as closed-shell hydrogen bonds or CT complexes. Although the donor−acceptor nature of the hydrogen bond has been a subject of discussion,[63,65,66] the spin density of FH···$BH_2^{\bullet}$ provides objective evidence for a CT interaction which does not depend on a particular energy decomposition scheme. In summary, we attribute the binding in the electron-rich and electron-deficient complexes studied to the presence of additional and/or stronger donor−acceptor interactions compared to closed-shell analogues, warranting further studies on radical−solvent interactions. The application of energy decomposition analysis based on localized orbitals,[31] in future studies, may provide further insight into the binding in radical−solvent complexes.

■ ASSOCIATED CONTENT

Supporting Information

Computational details; components of benchmark binding energies; a brief overview of the type of NLMO analysis used. This material is available free of charge via the Internet at http://pubs.acs.org.

■ AUTHOR INFORMATION

Corresponding Author

*E-mail: peter.tentscher@epfl.ch; samuel.arey@epfl.ch.

Notes

The authors declare no competing financial interest.

■ ACKNOWLEDGMENTS

This work was supported by the Swiss National Science Foundation (SNSF) ProDoc TM Grant PDFMP2-123028. We thank Hendrik Zipse for useful discussions. P.R.T. thanks Frank Weinhold for a hands-on introduction to NBO methods.

■ REFERENCES

(1) Augusto, O.; Bonini, M. G.; Amanso, A. M.; Linares, E.; Santos, C. C.; Menezes, S. L. D. Nitrogen Dioxide and Carbonate Radical Anion: Two Emerging Radicals in Biology. *Free Radic. Biol. Med.* **2002**, *32*, 841−859.

(2) Canonica, S.; Tratnyek, P. Quantitative Structure−Activity Relationships for Oxidation Reactions of Organic Chemicals in Water. *Environ. Toxicol. Chem.* **2003**, *22*, 1743−54.

(3) Zhao, J.; Zhang, R. Chapter 10 Theoretical Investigation of Atmospheric Oxidation of Biogenic Hydrocarbons: A Critical Review. *Adv. Quantum Chem.* **2008**, *55*, 177−213.

(4) Maciel, G. S.; Cappelletti, D.; Grossi, G.; Pirani, F.; Aquilanti, V. Chapter 15 Elementary Processes in Atmospheric Chemistry: Quantum Studies of Intermolecular Dimer Formation and Intramolecular Dynamics. *Adv. Quantum Chem.* **2008**, *55*, 311−332.

(5) Glowacki, D. R.; Pilling, M. J. Unimolecular Reactions of Peroxy Radicals in Atmospheric Chemistry and Combustion. *ChemPhysChem* **2010**, *11*, 3836−3843.

(6) Francisco, J. S.; Muckerman, J. T.; Yu, H.-G. HOCO Radical Chemistry. *Acc. Chem. Res.* **2010**, *43*, 1519−1526.

(7) Chałasiński, G.; Szczęśniak, M. M. State of the Art and Challenges of the *ab Initio* Theory of Intermolecular Interactions. *Chem. Rev.* **2000**, *100*, 4227−4252.

(8) Rudic, S.; Merritt, J. M.; Miller, R. E. Study of the CH_3H_2O Radical Complex Stabilized in Helium Nanodroplets. *Phys. Chem. Chem. Phys.* **2009**, *11*, 5345−5352.

(9) Sander, W.; Roy, S.; Polyak, I.; Ramirez-Anguita, J. M.; Sanchez-Garcia, E. The Phenoxyl Radical−Water Complex-A Matrix Isolation and Computational Study. *J. Am. Chem. Soc.* **2012**, *134*, 8222−8230.

(10) Gill, P. M. W.; Radom, L. Structures and Stabilities of Singly Charged Three-Electron Hemibonded Systems and Their Hydrogen-Bonded Isomers. *J. Am. Chem. Soc.* **1988**, *110*, 4931−4941.

(11) Bickelhaupt, F. M.; Diefenbach, A.; de Visser, S. P.; de Koning, L. J.; Nibbering, N. M. M. Nature of the Three-Electron Bond in H_2S-SH_2^+. *J. Phys. Chem. A* **1998**, *102*, 9549−9553.

(12) Clark, T. Odd-Electron σ Bonds. *J. Am. Chem. Soc.* **1988**, *110*, 1672−1678.

(13) Kim, H.; Lee, H. M. Ammonia−Water Cation and Ammonia Dimer Cation. *J. Phys. Chem. A* **2009**, *113*, 6859−6864.

(14) Bil, A.; Berski, S.; Latajka, Z. On Three-Electron Bonds and Hydrogen Bonds in the Open-Shell Complexes H_2X_2+ for X = F, Cl, and Br. *J. Chem. Inf. Model.* **2007**, *47*, 1021−1030.

(15) Lee, H. M.; Kim, K. S. Water Dimer Cation: Density Functional Theory vs Ab Initio Theory. *J. Chem. Theory Comput.* **2009**, *5*, 976−981.

(16) Maity, D. K. Sigma Bonded Radical Cation Complexes: A Theoretical Study. *J. Phys. Chem. A* **2002**, *106*, 5716−5721.

(17) Burcl, R.; Hobza, P. Ab Initio Study on the Methanol−Water Cation Radical Potential Energy Surface. *Theor. Chem. Acc.* **1993**, *87*, 97−105.

(18) Hobza, P.; Burcl, R.; Špirko, V.; Dopfer, O.; Müller-Dethlefs, K.; Schlag, E. W. Ab Initio Study of the Phenol−Water Cation Radical. *J. Chem. Phys.* **1994**, *101*, 990−997.

(19) Sodupe, M.; Oliva, A.; Bertran, J. Theoretical Study of the Ionization of the H_2O-H_2O, NH_3-H_2O, and FH-H_2O Hydrogen-Bonded Molecules. *J. Am. Chem. Soc.* **1994**, *116*, 8249−8258.

(20) Coitiño, E. L.; Lledos, A.; Serra, R.; Bertran, J.; Ventura, O. N. Ab Initio Study of the Structure and Reactivity of H_2CO-H_2O^+ and Related Radical Cations. *J. Am. Chem. Soc.* **1993**, *115*, 9121−9126.

(21) Coitiño, E. L.; Pereira, A.; Ventura, O. N. High-Level Ab Initio Prediction of the Structure and Infrared Spectra of Formaldehyde−Water Radical-Cation Complexes. *J. Chem. Phys.* **1995**, *102*, 2833−2840.

(22) Schulz, C. P.; Haugstätter, R.; Tittes, H. U.; Hertel, I. V. Free Sodium-Water Clusters. *Phys. Rev. Lett.* **1986**, *57*, 1703−1706.

(23) Hashimoto, K.; Morokuma, K. Ab Initio Molecular Orbital Study of $Na(H_2O)_n$ (n = 1−6) Clusters and Their Ions. Comparison of Electronic Structure of the "Surface" and "Interior" Complexes. *J. Am. Chem. Soc.* **1994**, *116*, 11436−11443.
(24) Yoder, B. L.; West, A. H. C.; Schlappi, B.; Chasovskikh, E.; Signorell, R. A Velocity Map Imaging Photoelectron Spectrometer for the Study of Ultrafine Aerosols with a Table-Top VUV Laser and Na-Doping for Particle Sizing Applied to Dimethyl Ether Condensation. *J. Chem. Phys.* **2013**, *138*, 044202 1−12.
(25) Yoder, B. L.; Litman, J. H.; Forysinski, P. W.; Corbett, J. L.; Signorell, R. Sizer for Neutral Weakly Bound Ultrafine Aerosol Particles Based on Sodium Doping and Mass Spectrometric Detection. *J. Phys. Chem. Lett.* **2011**, *2*, 2623−2628.
(26) Litman, J. H.; Yoder, B. L.; Schlappi, B.; Signorell, R. Sodium-Doping as a Reference to Study the Influence of Intracluster Chemistry on the Fragmentation of Weakly-Bound Clusters Upon Vacuum Ultraviolet Photoionization. *Phys. Chem. Chem. Phys.* **2013**, *15*, 940−949.
(27) Forysinski, P. W.; Zielke, P.; Luckhaus, D.; Corbett, J.; Signorell, R. Photoionization of Small Sodium-Doped Acetic Acid Clusters. *J. Chem. Phys.* **2011**, *134*, 094314 1−11.
(28) Ramaniah, L. M.; Bernasconi, M.; Parrinello, M. Density-Functional Study of Hydration of Sodium in Water Clusters. *J. Chem. Phys.* **1998**, *109*, 6839−6843.
(29) Hashimoto, K.; Kamimoto, T. Theoretical Study of Microscopic Solvation of Lithium in Water Clusters: Neutral and Cationic $Li(H_2O)_n$ (n = 1−6 and 8). *J. Am. Chem. Soc.* **1998**, *120*, 3560−3570.
(30) Cwiklik, L.; Buck, U.; Kulig, W.; Kubisiak, P.; Jungwirth, P. A Sodium Atom in a Large Water Cluster: Electron Delocalization and Infrared Spectra. *J. Chem. Phys.* **2008**, *128*, 154306 1−9.
(31) Horn, P. R.; Sundstrom, E. J.; Baker, T. A.; Head-Gordon, M. Unrestricted Absolutely Localized Molecular Orbitals for Energy Decomposition Analysis: Theory and Applications to Intermolecular Interactions Involving Radicals. *J. Chem. Phys.* **2013**, *138*, 134119 1−14.
(32) Tentscher, P. R.; Arey, J. S. Binding in Radical-Solvent Binary Complexes: Benchmark Energies and Performance of Approximate Methods. *J. Chem. Theory Comput.* **2013**, *9*, 1568−1579.
(33) For $NH_3^{\bullet+}$, the spin-bearing N interacting with the water lone pairs soes not correspond to the global minimum, the latter being an H-bonded complex.[13,32]
(34) Weinhold, F.; Landis, C. *Discovering Chemistry with Natural Bond Orbitals*; Wiley: New York, 2012.
(35) Weinhold, F. In *Encyclopedia of Computational Chemistry*; Schleyer, P. v. R., Allinger, N. L., Clark, T., Gasteiger, J., Kollman, P. A., Schaefer, H. F., III, Schreiner, P. R., Eds.; John Wiley & Sons: New York, 1998; Chapter Natural Bond Orbital Methods, pp 1792−1811.
(36) Glendening, E. D.; Landis, C. R.; Weinhold, F. Natural Bond Orbital Methods. *WIREs Comput. Mol. Sci.* **2012**, *2*, 1−42.
(37) Reed, A. E.; Weinhold, F. Natural Localized Molecular Orbitals. *J. Chem. Phys.* **1985**, *83*, 1736−1740.
(38) Weinhold, F.; Landis, C. *Valency and Bonding: A Natural Bond Orbital Donor-Acceptor Perspective*; Cambridge University Press: Oxford, UK, 2003.
(39) Reed, A. E.; Weinstock, R. B.; Weinhold, F. Natural Population Analysis. *J. Chem. Phys.* **1985**, *83*, 735−746.
(40) Mayer, I. Bond Order and Valence Indices: A Personal Account. *J. Comput. Chem.* **2007**, *28*, 204−221.
(41) We refer to eqs (44) and (46) in ref 40. The given values were computed from Wiberg bond indices (WBIs) in the NAO basis, computed as $B_{AB} = 2{\cdot}WBI_{\alpha} + 2{\cdot}WBI_{\beta}$.
(42) Hund, F. Zur Deutung der Molekelspektren. IV. *Z. Physik* **1928**, *51*, 759−795.
(43) Carpenter, J.; Weinhold, F. Analysis of the Geometry of the Hydroxymethyl Radical by the "Different Hybrids for Different Spins" Natural Bond Orbital Procedure. *J. Mol. Struct.-Theochem* **1988**, *169*, 41−62.
(44) Watts, J. D.; Gauss, J.; Bartlett, R. J. Open-Shell Analytical Energy Gradients for Triple Excitation Many-Body, Coupled-Cluster Methods: MBPT(4), CCSD+T(CCSD), CCSD(T), and QCISD(T). *Chem. Phys. Lett.* **1992**, *200*, 1−7.
(45) Dunning, T. H., Jr. Gaussian Basis Sets for Use in Correlated Molecular Calculations. I. The Atoms Boron Through Neon and Hydrogen. *J. Chem. Phys.* **1989**, *90*, 1007−1023.
(46) Woon, D. E.; Dunning, T. H., Jr. Gaussian Basis Sets for Use in Correlated Molecular Calculations. III. The Atoms Aluminum Through Argon. *J. Chem. Phys.* **1993**, *98*, 1358−1371.
(47) Peterson, K. A.; Dunning, T. H., Jr. Accurate Correlation Consistent Basis Sets for Molecular Core−Valence Correlation Effects: The Second Row Atoms Al−Ar, and the First Row Atoms B-Ne Revisited. *J. Chem. Phys.* **2002**, *117*, 10548−10560.
(48) Watts, J. D.; Bartlett, R. J. The Coupled-Cluster Single, Double, and Triple Excitation Model for Open-Shell Single Reference Functions. *J. Chem. Phys.* **1990**, *93*, 6104−6105.
(49) Bomble, Y. J.; Stanton, J. F.; Kállay, M.; Gauss, J. Coupled-Cluster Methods Including Noniterative Corrections for Quadruple Excitations. *J. Chem. Phys.* **2005**, *123*, 054101 1−8.
(50) Cowan, R. D.; Griffin, D. C. Approximate Relativistic Corrections to Atomic Radial Wave Functions. *J. Opt. Soc. Am.* **1976**, *66*, 1010−1014.
(51) Faas, S.; Snijders, J.; van Lenthe, J.; van Lenthe, E.; Baerends, E. The ZORA Formalism Applied to the Dirac-Fock Equation. *Chem. Phys. Lett.* **1995**, *246*, 632−640.
(52) Stanton, J. F.; Gauss, J.; Harding, M. E.; Szalay, P. G. with contributions from Auer, A. A.; Bartlett, R. J.; Benedikt, U.; Berger, C.; Bernholdt, D. E.; Bomble, Y. J.; Cheng, L.; Christiansen, O.; Heckert, M.; Heun, O.; Huber, C.; Jagau, T.-C.; Jonsson, D.; Jusélius, J.; Klein, K.; Lauderdale, W. J.; Matthews, D. A.; Metzroth, T.; Mück, L. A.; O'Neill, D. P.; Price, D. R.; Prochnow, E.; Puzzarini, C.; Ruud, K.; Schiffmann, F.; Schwalbach, W.; Stopkowicz, S.; Tajti, A.; Vázquez, J.; Wang, F.; Watts J. D. and the integral packages MOLECULE (Almlöf, J.; Taylor, P. R.), ABACUS (Helgaker, T.; Jensen, H.J.Aa.; Jørgensen, P.; Olsen, J.), and ECP routines by Mitin, A. V.; van Wüllen, C. For the current version, see http://www.cfour.de (accessed November 2011).
(53) Schaftenaar, G.; Noordik, J. Molden: a Pre- and Post-Processing Program for Molecular and Electronic Structures. *J. Comput.-Aided Mol. Des.* **2000**, *14*, 123−134.
(54) Frisch, M. J.; Trucks, G. W.; Schlegel, H. B.; Scuseria, G. E.; Robb, M. A.; Cheeseman, J. R.; Scalmani, G.; Barone, V.; Mennucci, B.; Petersson, G. A.; Nakatsuji, H.; Caricato, M.; Li, X.; Hratchian, H. P.; Izmaylov, A. F.; Bloino, J.; Zheng, G.; Sonnenberg, J. L.; Hada, M.; Ehara, M.; Toyota, K.; Fukuda, R.; Hasegawa, J.; Ishida, M.; Nakajima, T.; Honda, Y.; Kitao, O.; Nakai, H.; Vreven, T.; Montgomery, J. A., Jr.; Peralta, J. E.; Ogliaro, F.; Bearpark, M.; Heyd, J. J.; Brothers, E.; Kudin, K. N.; Staroverov, V. N.; Kobayashi, R.; Normand, J.; Raghavachari, K.; Rendell, A.; Burant, J. C.; Iyengar, S. S.; Tomasi, J.; Cossi, M.; Rega, N.; Millam, J. M.; Klene, M.; Knox, J. E.; Cross, J. B.; Bakken, V.; Adamo, C.; Jaramillo, J.; Gomperts, R.; Stratmann, R. E.; Yazyev, O.; Austin, A. J.; Cammi, R.; Pomelli, C.; Ochterski, J. W.; Martin, R. L.; Morokuma, K.; Zakrzewski, V. G.; Voth, G. A.; Salvador, P.; Dannenberg, J. J.; Dapprich, S.; Daniels, A. D.; Farkas, O.; Foresman, J. B.; Ortiz, J. V.; Cioslowski, J.; Fox, D. J. *Gaussian 09*, revision B.1; Gaussian Inc.: Wallingford CT, 2009.
(55) Kendall, R. A.; Dunning, T. H., Jr.; Harrison, R. J. Electron Affinities of the First-Row Atoms Revisited. Systematic Basis Sets and Wave Functions. *J. Chem. Phys.* **1992**, *96*, 6796−6806.
(56) Becke, A. D. A New Mixing of Hartree−Fock and Local Density-Functional Theories. *J. Chem. Phys.* **1993**, *98*, 1372−1377.
(57) Glendening, E. D.; Badenhoop, J. K.; Reed, A. E.; Carpenter, J. E.; Bohmann, J. A.; Morales, C. M.; Weinhold, F. *NBO 5.0.*; Theoretical Chemistry Institute, University of Wisconsin: Madison, 2001.
(58) Shao, Y.; Molnar, L. F.; Jung, Y.; Kussmann, J.; Ochsenfeld, C.; Brown, S. T.; Gilbert, A. T.; Slipchenko, L. V.; Levchenko, S. V.; O'Neill, D. P.; et al. Advances in Methods and Algorithms in a Modern Quantum Chemistry Program Package. *Phys. Chem. Chem. Phys.* **2006**, *8*, 3172−3191.

(59) Boese, A. D.; Martin, J. M. L.; Klopper, W. Basis Set Limit Coupled Cluster Study of H-Bonded Systems and Assessment of More Approximate Methods. *J. Phys. Chem. A* **2007**, *111*, 11122−11133.
(60) Makarewicz, J. Ab Initio Intermolecular Potential Energy Surfaces of the Water−Rare Gas Atom Complexes. *J. Chem. Phys.* **2008**, *129*, 184310 1−10.
(61) Natural population analysis charges on C in CF^{+} and $CO^{\bullet+}$ were within 0.1 of each other.
(62) A STERIC analysis withing the NBO framework could provide some insight regarding the strength of the steric repulsion. However, such an analysis should be carried out at the HF level of theory, which describes the hemibonded complexes of our previous study[32] unsatisfactorily; hence we did not report such data.
(63) Grabowski, S. J. What Is the Covalency of Hydrogen Bonding? *Chem. Rev.* **2011**, *111*, 2597−2625.
(64) Hernández-Soto, H.; Weinhold, F.; Francisco, J. S. Radical Hydrogen Bonding: Origin of Stability of Radical-Molecule Complexes. *J. Chem. Phys.* **2007**, *127*, 164102 1−10.
(65) Weinhold, F. In *Peptide Solvation and H-Bonds*; Baldwin, R. L., Baker, D., Eds.; Advances in Protein Chemistry; Academic Press: Waltham, MA, 2005; Vol. 72; pp 121 − 155.
(66) Khaliullin, R.; Bell, A.; Head-Gordon, M. Electron Donation in the Water−Water Hydrogen Bond. *Chem.—Eur. J.* **2009**, *15*, 851−855.